Influence of surfactant concentration on drop production by bubble bursting

Juliette Pierre,* Mathis Poujol, and Thomas Séon
Sorbonne Université, CNRS, UMR 7190, Institut Jean Le Rond ∂'Alembert, F-75005 Paris, France

(Received 3 December 2021; accepted 22 June 2022; published 22 July 2022)

Bubbles bursting at the surface of the sea water produce drops and is the main source of sea spray aerosol. The mechanisms underlying the drops production from a single bubble bursting event have been intensively studied and the influence of the bubble size and liquid parameters (density, viscosity, and surface tension) has been unified. However, despite the diversity of the surfactant molecules present in the oceans, their influence has been overlooked. In this paper we experimentally explore the influence of the surfactant concentration [sodium dodecyl surfate (SDS)] in a water solution on a single bubble collapse and subsequent drop production. We show that these surfactant molecules have an astonishing effect. In particular, we quantitatively show that they modify the bubble collapse, they induce less, smaller, and faster drops, and they can even completely prevent the drop production for a particular concentration. These results allow us to affirm that these important effects are mainly a consequence of the local surface tension gradients (Marangoni stresses), more than just the surface tension lowering, and to the related nonmonotonic variation of the surface elasticity with the surfactant concentration. Finally, this study shows that the role of water contamination by surface-active agents is important and needs to be understood to improve the prediction of the sea spray aerosol.

DOI: 10.1103/PhysRevFluids.7.073602

I. INTRODUCTION

As a wave crashes in the ocean it entrains air below the surface. After a turbulent break-up cascade [1] a population of bubbles is produced [2–4] and while small bubbles may be dissolved into the water, larger bubbles rise back to the surface and collapse [5]. The bursting of a bubble starts with the break up of the thin liquid film that separates the air cavity from the atmosphere and ends up with the fragmentation of a rising jet. Through these two fragmentation events, bubble bursting produces film drops [6,7] and jet drops [8–13] and constitutes one of the main sources of the ocean spray [14]. By evaporating, the sea spray transports in the atmosphere water vapor, important for the thermodynamics of the atmosphere, and salt crystals that affect the radiative balance of the atmosphere and form cloud condensation nuclei [15,16]. And, in a significant way, they carry also heat, dissolved gases, surfactants, biological materials [5]. Finally, uncertainties in predicting sea spray aerosols characteristics directly impacts our ability to perform weather prediction and earth system modeling [17,18].

Since the pioneer work of D. Blanchard [19] there have been a number of—experimental, numerical and theoretical—combining studies on a single bubble bursting, that brought comprehensive data on the size and speed of the jet drops produced by bubble bursting in water [20–23]. Applying these results to the bubble size distribution produced under a breaking wave enabled a rough estimation of the statistics of jet drop production [24]. However, the ocean surface is partly covered by a biofilm, which can be modeled with surfactants [25]. The surface-active contaminations are

*juliette.pierre@sorbonne-universite.fr

known to modify the static and dynamic behaviors of bubbles, including their coalescence, lifetimes, and bursting [26–28]. Consequently, the influence of the physicochemistry of the interface has to be taken into account in the process of bubble collapse at the interface and in the subsequent drop production. Néel and Deike (2021) [28] considered a monodisperse assembly of millimetric air bubbles produced identically in the bulk for a wide range of surface contamination and showed that, depending on the contamination, the bubble distribution that bursts can be very distinct from the initial distribution. Following on from this study they reveal an optimal production regime of droplets during collective bubble bursting in contaminated water with a low concentration of surfactant [29]. There have been various experiments that attempted to described the role of the physicochemical parameters on the production of droplets by bursting bubbles [3,5,30,31], but there are large variations in protocols, and the influence of surfactants on the drop production remains largely unclear. All these experiments are realized on a large collection of bubbles, with different size distributions, suggesting the need to carry out a study on a single bursting bubble. Recently, Constante-Amores *et al.* (2021) [32] studied the effect of surfactant on the dynamics of a bubble bursting, using numerical simulations, accounting for sorption kinetics and diffusive effects. At one fixed bubble size and one surface contamination, they showed that the presence of surfactant affects the dynamics of the system through Marangoni-induced flow and is responsible for delaying the collapse and generating slower and fewer drops.

In this article, we study experimentally the effect of sodium dodecyl sulfate (SDS) surfactant on the dynamics of a bubble bursting through an interface. After describing the experimental setup, we show qualitatively that the surfactants have an astonishing influence on the jet dynamics subsequent to the bubble collapse, and on the jet drops production. The following is dedicated to quantify this effect by varying the surfactant concentration and the bubble size. We start by studying the influence of the surfactants on the bubble collapse time, before characterizing the variation of the number, size and speed of the ejected drops as a function of the control parameters. Finally, we focus on the influence of the surfactant concentration on the cavity collapse and the capillary waves dynamics. We show that surfactants have a striking effect on the bubble bursting process because both, surfactants transport and bubble bursting, have dynamics with similar timescales and, thus, surface elasticity plays a crucial role.

II. EXPERIMENTAL SETUP

The experiment consists in releasing a single air bubble from a submerged needle in a liquid and recording the upward jet and released drops after the bubble bursts at the free surface. Air bubbles are generated in a parallelipedal glass tank (20 cm length, 14 cm width, 9.5 cm depth) filled with either tap water or an aqueous solution of SDS (purchased from Sigma Aldrich) surfactant with a mass concentration ranging from 0.5 to 10 g/l, i.e., 1.7 to 34.7 mM. For SDS at the ambient temperature the critical micelle concentration (CMC) is found to be around 8 mM [33], which means that the SDS concentration in our solutions varies from C = 0.2 CMC to 4.3 CMC. Bubbles are generated using a syringe pump filled with air. Three different needles are used, with internal diameter varying from 0.8 to 1.5 mm enabling to create bubble with thee different radii: 0.8, 1.1, 1.7 $\pm$ 0.1 mm. The bubbles rise to the surface and briefly float before bursting. Considering the ellipsoidal shape of the floating bubble, we defined an equivalent radius as $R = (a^2 b)^{1/3}$ with a and b respectively the semimajor and semiminor axes of the ellipsoid. The surface tension of each solution is measured using the pendant drop technique [34].

In all experiments a digital high speed camera (*Phantom* V2511) is used at 100 000 frames per second with a 12$\times$ zoom lens system to image the rising jet and releasing drops from the side, above the free surface. In a few experiments, a second digital high speed camera (*Photron* SA-5) is added to image at 10 000 frames per second with a macro lens the collapse of the submerged cavity below the free surface.

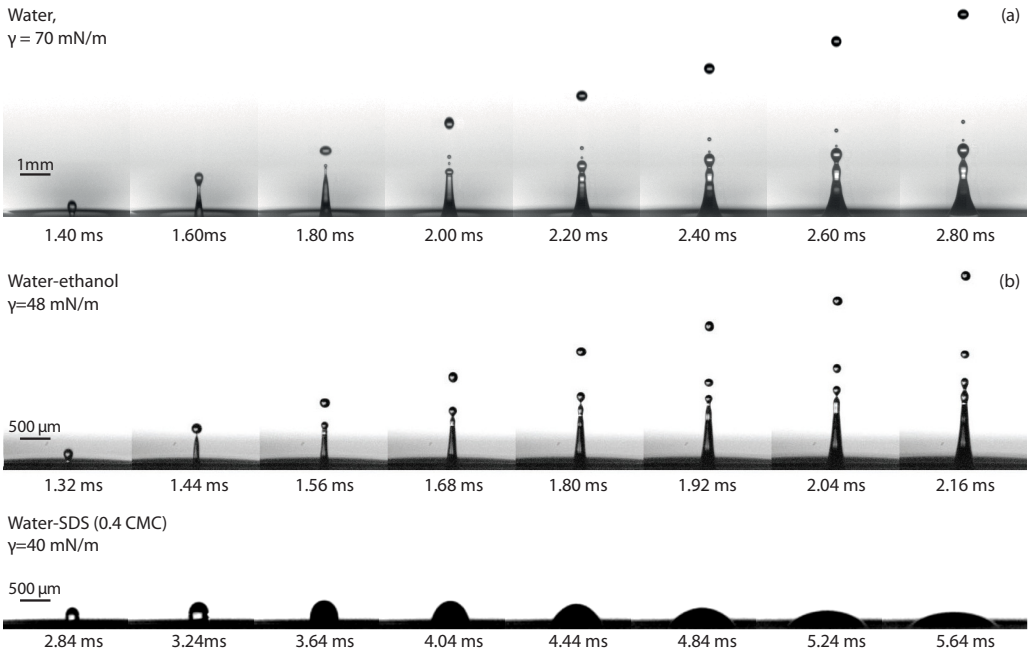

FIG. 1. Sequences of bursting bubbles (bubbles start to burst at 0 ms) with comparable radius in three different liquids : (a) water, $\gamma = 70$ mN m^{-1}, $R = 830$ μm; (b) water-ethanol solution with respectively 89.5% and 10.5% of total weight, $\gamma = 48$ mN m^{-1}, $R = 830$ μm; (c) water-SDS solution with 3.4 mM of SDS, $\gamma = 40$ mN m^{-1}, $R = 840$ μm. The surfactants have a strong influence on the jet dynamics, independently of their influence on the surface tension. The time and space scales of the sequences (a) and (b) have been chosen to show the similarity between the two dynamics.

III. QUALITATIVE DESCRIPTION

Figure 1 presents three sequences of bubble busting. In each case the bubble radius is almost constant and the liquid is different : (a) tap water ($\gamma = 70$ mN m^{-1}), (b) a water-ethanol mixture with a surface tension $\gamma = 48$ mN m^{-1}, and (c) a water-SDS solution with a surface tension $\gamma = 40$ mN m^{-1}. We observe on Figs. 1(a) and 1(b) that the decrease of surface tension does not affect much the drop size and velocity. These observations have been reported quantitatively in the literature [9,11,20–22]. In the sequence Fig. 1(c), the bubble bursts in a liquid with surfactants concentrated at 0.4 CMC and with a surface tension very close to that of sequence Fig. 1(b). The result is remarkable. The presence of surfactants completely changes the jet dynamics, the jet velocity is so low that it can barely reach the free surface and cannot produce any droplet. In the following, our goal is to examine more quantitatively the influence of the surfactant concentration on the drop dynamics, and to look at where and how, in the cavity collapse process, the surfactants can have such a strong influence.

IV. THE BUBBLE COLLAPSE

Before the cavity collapses, the bubble is floating at the free surface. As it is static, its shape is due to an equilibrium between capillarity and gravity and is obtained by integration of the Young–Laplace equation [7,35,36]. Surfactants have no more influence on the static bubble shape than through their modification of the surface tension. Consequently, the static bubble shape before bursting cannot be responsible for the modification of the jet dynamics between Figs. 1(b) and 1(c).

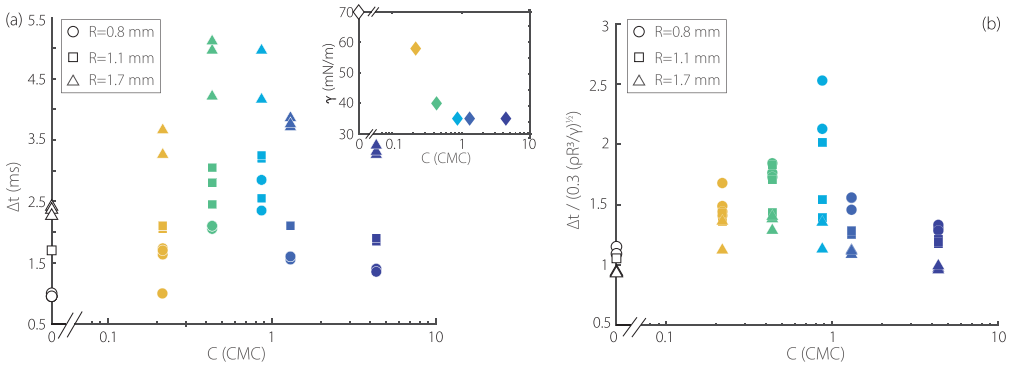

FIG. 2. (a) Bubble collapsing time Δt for three different bubble radii $R = 0.8 \pm 0.1$ mm (circle), 1.1 ± 0.1 mm (square) and 1.7 ± 0.1 mm (triangle), as a function of the surfactant concentration, adimensionalized using the critical micelle concentration (CMC). The CMC is taken equal to 8 mM [33]. Inset: for each solution the surface tension is measured using the pendant drop technique and reported as a function of the surfactant concentration. (b) Collapsing time, Δt, normalized by the capillaro-inertial timescale, $\sqrt{\rho R^3/\gamma}$, as a function of the dimensionless surfactant concentration, for three different bubble radii $R = 0.8 \pm 0.1$, 1.1 ± 0.1 and 1.7 ± 0.1 mm. The 0.3 prefactor is added in the normalization of Δt to have the dimensionless collapsing time equal to one. The color of the markers is associated to the surfactant concentration in the liquid.

We then focus on the influence of the surfactant concentration on the bubble collapse duration Δt. Δt is defined as the time elapsed between the hole nucleation in the cap film and the cavity reversal, when the depth of the immersed cavity starts to decrease. Figure 2(a) presents Δt for three different bubble radii R = 0.8 mm (circle), 1.1 mm (square), and 1.7 mm (triangle), as a function of the surfactant concentration adimensionalized using the CMC, C(CMC). The color of the markers is associated to the surfactant concentration in the liquid. Note that the same markers at one concentration show Δt for experiments in similar conditions, they therefore reflect the dispersion of the results. We observe that, independently of the dispersion, the bubble collapsing time always increases with the surfactant concentration, reaches a maximum close to the CMC and decreases. In other words, up to the CMC, the cavity becomes slower to collapse as the surfactants are more concentrated and, above the CMC, it becomes faster again. This nonmonotonic variation of the collapsing time with the surfactant concentration can be surprising. In particular because the variation of the surface tension γ with the dimensionless surfactant concentration C is monotonic, as verified in the inset where γ expectedly decreases with C, from the water surface tension, until it reaches a plateau, around 36 mN/m, beyond the CMC. Consequently, the nonmonotonic variation of Δt with C indicates that the surfactant dynamics should play a role in the cavity collapse.

In this capillaro-inertial collapse, Δt is expected to scale as the capillaro-inertial time: $\sqrt{\rho R^3/\gamma}$, with ρ the liquid density and R the bubble radius [36]. Figure 2(b) presents the collapsing time Δt normalized by this capillaro-inertial timescale as a function of the dimensionless surfactant concentration C, for the three different bubble radii $R = 0.8$, 1.1, and 1.7 mm. As expected, without surfactant ($C = 0$), all the bubbles with different radius collapse, demonstrating that this adimensionalized collapsing time is relevant and that the collapsing dynamics is the result of the balance between inertia and capillarity, where the effect of capillarity is well quantified by the value of the surface tension. The prefactor 0.3 is added to the capillaro-inertial time so that the normalized times collapse around 1. However, the data do not rescale anymore when surfactants are added to the water, pointing out that the effect of the surfactant is different than just changing the surface tension. Moreover, increasing the surfactant concentration increases this effect of spreading of the adimensionalized data. This means that the influence of the surfactants in the collapsing dynamics increases with their concentration. This surfactant effect is maximum close to the CMC

(blue markers) and then it decreases again. The value of the dimensionless collapsing time follow the same nonmonotonic variation as the collapsing time in Fig. 2(a).

By normalizing Δt by the relevant capillaro-inertial collapsing time, Fig. 2(b) enables to decorrelate the respective influence of the surface tension and the surfactant dynamics. As the data do not rescale in the presence of the surfactants, they are expected to be a consequence of the particular dynamics of the surfactants, independently of their influence on the measured liquid surface tension γ displayed in the inset. Indeed, in processes that involve surface stretching and/or capillary waves, as it is the case in our experiment, gradients of surfactants can appear, generating Marangoni stresses that affect the dynamics [37,38]. Constante-Amores *et al.* [32] showed that in the insoluble surfactant limit, the collapse yields to an over-concentration of surfactants at the apex of the cavity when the capillary waves focus, source of a strong Marangoni stress that can delay the cavity collapse. In our cavity collapse experiment with soluble surfactants, such surfactant gradients can be generated at the surface, creating gradients of surface tension and thus surface elasticity. Depending on the competition between surface/bulk surfactant dynamics and surfactant advection at the free surface during the cavity collapse, the surface elasticity can be either unchanged, nonmonotonic with a maximum close to the CMC or monotonic and maximal above the CMC [39,40]. In our case, the nonmonotonic variation of Δt with the surfactant concentration observed in Fig. 2 strongly suggests that surface elasticity varies non monotonously with a maximum close to the CMC. Thus, surfactant advection along the surface and surface/bulk surfactant transport should both play a role by having similar characteristic times.

Consequently, in the aim of interpreting our results and contextualizing them within the existing literature, we need to discuss the surfactant dynamics in our experiment. Two surfactant kinetics must be considered and compared to its advection along the surface due to the cavity collapse: the surfactant surface diffusivity and its rearrangement between the surface and the bulk. First, the surface diffusivity D_s of SDS is around 10^{-9} m^2 s^{-1} [41]. Thus, the Peclet number $\mathrm{Pe} = \sqrt{\gamma R/\rho}/D_s$ that measures the relative importance of surface advection of surfactant to its diffusion is $\mathcal{O}(10^4)$ in our experiment. The surfactant surface diffusion is therefore not strong enough to mitigate its advection. Second, to estimate the surfactant rearrangement time between the surface and the bulk we need to compare the characteristic time of the sorption rates to the diffusion time of the surfactants. The Langmuir model gives the characteristic time for the sorption kinetics: $\tau_b = \Gamma_m/(k_{\mathrm{des}}\Gamma_m + k_{\mathrm{ads}}C)$ with $\Gamma_m = 4.10^{-6}$ mol m^{-2} [42] the maximum surface packing concentration of SDS at the air-water interface and k_{des} and k_{ads} respectively the desorption and adsorption rate [43]. The typical surface/bulk diffusion timescale can be expressed as $t_{\mathrm{diff}} = \Gamma^2/(D_v C^2)$ with Γ the surface concentration at equilibrium, defined as $\Gamma = (k_{\mathrm{ads}}C/k_{\mathrm{des}})(1 - \Gamma/\Gamma_m)$ [44] and $D_v = 5.10^{-10}$ m^2 s^{-1} [45] the diffusion coefficient of the surfactants in the bulk liquid. The characteristic time τ_b is not easy to estimate, in particular due to the lack of precision in the sorption rates k_{des} and k_{ads}. By using the values of k_{des} and k_{ads} measured in the literature [43], the diffusion time, of the order of the millisecond, seems to remain larger than the time of the adsorption-desorption kinetics. This indicates that the dynamics of surfactants is limited by the diffusion, which is of the same order of magnitude than the time of collapse Δt.

Consequently, these estimations of the characteristic times of surfactant dynamics confirm our interpretation of Fig. 2: the nonmonotonic variation of the collapsing time Δt with the surfactant concentration C is a consequence of the nonmonotonic surface elasticity variation with the surfactant concentration. This solubility effect of our surfactant is important in this experiment because both its surface/bulk transport and advection along the surface by cavity collapse have similar timescales. This makes this experiment very sensitive to the presence of surfactant, which will be confirmed in the next section.

V. JET DROPS CHARACTERISTICS

As shown in Fig. 1, after a bubble has collapsed, an upward jet usually rises and produces the so-called jet drops. Figure 3(a) presents the number of these drops produced when a bubble bursts,

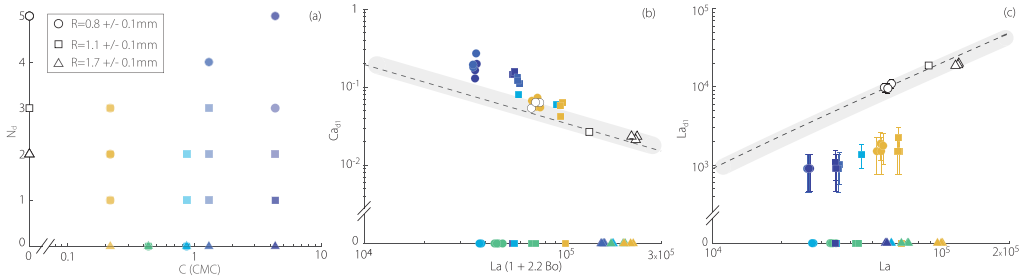

FIG. 3. (a) Number of ejected drops as a function of the SDS concentration. The opacity of the symbols has been decreased so that the superposition of symbols appears darker and every data point can be seen. (b) Capillary number of the first ejected drop as a function of La(1+2.2Bo). The dashed line represents the relation : $\mathrm{Ca}_{d1} = 19(1 + 2.2\mathrm{Bo})^{-3/4}\mathrm{La}^{-3/4}(500^{-1/2} - \mathrm{La}^{-1/2})^{-3/4}$ used in Ref. [22] [Eq. (5)] and in Ref. [46] [Eq. (6)] and based on the scaling law proposed by Gañán-Calvo (2017) [12]. (c) Laplace number of the first ejected drop as function of the Laplace number of initial bubble. The dashed line represents the scaling proposed by Gañán-Calvo (2017) [12]: $\mathrm{La}_{d1} = 0.6[\sqrt{\mathrm{La}}(\sqrt{\mathrm{La}/500} - 1)]^{5/4}$ and already used in Ref. [22] [Eq. (7)]. In all graphs color codes for the SDS concentration and symbol codes for the bubble size. The thickness of the grey zone simply reproduces the dispersion of the experimental and numerical values appearing in the corresponding figures of Berny *et al.* [22].

as a function of the surfactant concentration, for three different bubble radii. For bubbles bursting in water (C = 0, empty markers) the three different bubbles produce droplets and the smaller the bubble, the more drops are produced [22]. When surfactants are added to the water, our largest bubble size (triangle) cannot produce drop anymore, regardless of the surfactant concentration tested. This is a strong result, for this bubble size, surface contamination completely kills the drop production. Then, for smaller bubble, we observe that there is dispersion in the number of produced droplets. Indeed, for $\mathrm{C} \simeq 0.2$ (yellow markers), R = 0.8 and 1.1 mm are superimposed and produce either 1, 2, or 3 droplets. There is the same kind of dispersion for $\mathrm{C} \geqslant 0.9$ Nevertheless, despite this dispersion, the trend is clear: (i) surface contamination can prevent the drop production and (ii) when droplets are produced there are less numerous and their number seems to decrease down to a minimum around half the CMC, before increasing again. These results are crucial, they signify that the size distribution of ejected jet drops produced in pure water [24] might be very different than the one produced in water with surfactant. They precise and experimentally validate the recent numerical results of Constante-Amores *et al.* [32] that show that a reduction in the number of ejected droplets arises with surfactant-laden flow due to Marangoni flow.

To go further in influence of the surfactant contamination in the jet drop production, the speed and size of the first ejected droplet are quantified as a function of the surfactant concentration. The first drop velocity is measured when it is detached [47]. Based on a large amount of numerical and experimental results, previous studies have demonstrated that the problem has two control parameters : the main one, the Laplace number (La), which compares the capillaro-inertial forces with the viscous forces, and the Bond number (Bo), which compares the gravitational forces with the capillary ones [12,21,22,46]. They are defined as

$$\mathrm{La} = \frac{\rho\gamma R}{\mu^2}, \tag{1}$$

$$\mathrm{Bo} = \frac{\rho g R^2}{\gamma}, \tag{2}$$

where R is the bubble radius, μ the liquid viscosity, ρ the liquid density, γ the surface tension, and g the acceleration of gravity. The first drop speed V_d and size R_d are also adimensionalized

using, respectively, the viscocapillary velocity $V_\mu = \gamma/\mu$ and length $l_\mu = \mu^2/(\rho\gamma)$, yielding the dimensionless drop speed and size:

$$\mathrm{Ca}_d = \frac{V_d \mu}{\gamma}, \tag{3}$$

$$\mathrm{La}_d = \frac{\rho\gamma R_d}{\mu^2}. \tag{4}$$

Within this dimensionless framework, previous studies [22,46] have proposed universal rescalings able to fully describe the first drop velocity and size. These scalings are respectively represented with dashed line on Figs. 3(b) and 3(c). They gather a large range of bubble size and liquid parameters (ρ, μ, γ). The thickness of the grey zone around the dashed line reproduces the dispersion of the experimental and numerical values appearing in the corresponding figures of Berny *et al.* [22]. The Bond number appears in the x-axis as a correction term for the drop velocity (Ca_d) and plays no role for the drop size (La_d).

On these plots we add here the values measured with bubbles bursting in our solutions of SDS mixed to water. The surfactant concentration is represented using the same colors as in Figs. 2 and 3(a). Expectedly, the drop velocity and size from bubble busting in water, with empty markers, fall onto the universal scalings. Moreover, many markers are on the x axis because no drop are produced for the largest bubble and for the concentration close to half of the CMC, as shown in Fig. 3(a). Then, in Fig. 3(b), we observe that the more concentrated is the solution, the higher the drop velocity is above the scaling. In Fig. 3(c), even with a small amount of surfactant, the drop size falls quite far below the universal scaling, and then it barely varies with the concentration or the Laplace number. In particular, for a given concentration there is no measurable dependency of the drop size with the Laplace number.

Here again, as for the cavity collapse, the surfactants have a strong influence on the jet dynamics and consequently on the drop production. Surfactants and jet dynamics have therefore similar timescales. However, the unexpected variations of the drop size and velocity indicate that the influence of the surfactants is highly non trivial, undoubtedly dependent on the local gradient concentration along the jet. Finally, we observe again that the dispersion is quite larger than without surfactant, may be because the dynamics is very sensitive to the balance between the coupled dynamics of the surfactant and the jet. The next step of this study will need a statistical characterization to properly capture the influence of the surfactant concentration in the drop production. The numerical simulation constitutes an efficient tool to realize this statistical study as it has been shown in previous studies on bubble bursting [24,48].

VI. CAPILLARY WAVES FOCUSING

The jet dynamics strongly depends on the capillary waves focusing at the bottom of the cavity [9,49]. Figure 4 presents three sequences of cavity collapse with almost the same bubble radius and three different surfactant concentrations: (a) no surfactant, (b) 0.4 CMC, and (c) 4.3 CMC. The capillary waves propagation is different in these three sequences. In particular, we see again, as in Fig. 2, that the capillary waves collapse more slowly with surfactant, but here we observe that the ratio between capillary wave propagation velocity and the hole opening changes: When the cavity reverses with surfactant on the last image of the sequences, the hole is larger. This changes the whole shape of the cavity. But the clearest difference lies in the wave shape itself, between Figs. 4(a) and 4(b), in particular in the second half of the collapse sequences. The shape of the lowest collapsing cavity shown in the second to last images is completely different, and undoubtedly explains the strong difference in the drop production dynamics (see $C = 0.4$ in Fig. 3). As shown by Constante-Amores *et al.* [32] for precise values of the control parameters, the interfacial surfactant concentration reaches its maximum value as the surfactant-laden capillary waves converge on the cavity apex. The Marangoni stresses that drive motion from high to low surface concentration regions can explain the wave shape.

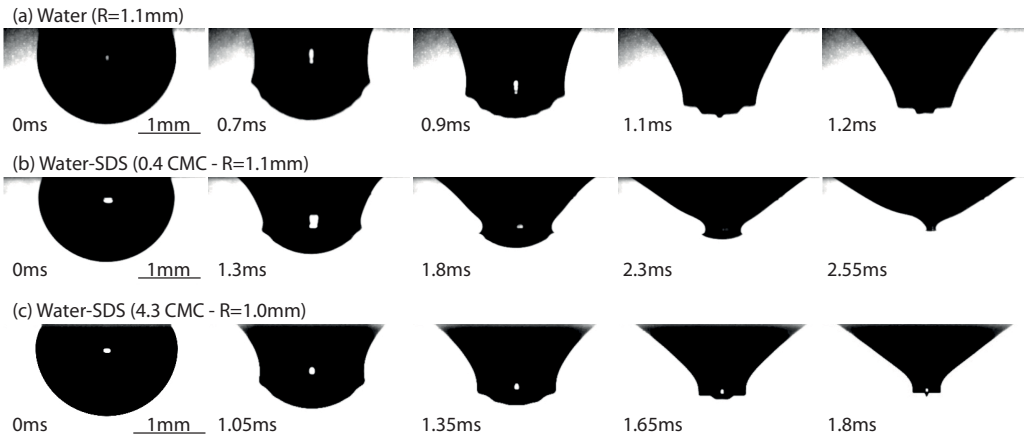

FIG. 4. Sequences showing the collapse of the submerged cavity for bubbles with almost the same radius in three different liquids: (a) water, $\gamma = 70\,\mathrm{mN\,m^{-1}}$, $R = 1.1\,\mathrm{mm}$, (b) water-SDS solution at 0.4 CMC, $R = 1.1\,\mathrm{mm}$, and (c) water-SDS solution at 4.3 CMC, $R = 1.0\,\mathrm{mm}$. The timescale of the three sequences has been chosen to compare the whole dynamics of the collapsing cavity, from cap film rupture up to cavity reversal.

For the highest concentration (c) the shape of the capillary waves, and of the lowest cavity, looks quite similar to the one in water. This seems to indicate that for concentration higher than the CMC, the Marangoni stresses are lower, due to lower concentration gradient, and this can be explained by a smaller diffusive time of the surfactants for high concentration that mitigates the local concentration gradients generated by the waves propagation. This similarity in the cavity collapse between no contamination and high contamination probably explains why the drop characteristics are closer between water and the highest concentration than water and 0.4 CMC, for which there is no drop produced.

VII. CONCLUSION

Surfactants are most often present in the liquids where bubbles are bursting (ocean, sparkle wine, soda...) and have barely been taken into account in the experiments and the models. In particular, to our knowledge, experiments of a single bubble bursting in a surfactant laden liquid have never been carried out. Here, we have shown how the SDS strongly influences the cavity collapse and the drops production, for different values of the bubble size and of the surfactant concentration. In particular, we highlight that the contamination induces: (i) a maximum in the bubble collapse duration around the CMC, (ii) smaller and faster drops, and (iii) less drops, with no drop at all for a particular concentration of half the CMC. An important result is that surfactants have such a striking effect on the bubble bursting process because both, surfactants and bubble bursting, have dynamics with similar timescales. This enables the surface elasticity to have a maximum close to the CMC and thus explains the nonmonotonic behavior we observe in the bubble collapse and drop production. The exact role of the local Marangoni flows is not known and needs to be clarified by quantifying the surface tension gradients appearing during the bubble collapse.

In the following, motivated by this study, more experiments should be done, in particular, with insoluble surfactants to examine the influence of the solubility. As it is complex to only change one parameter at a time, it would undoubtedly be interesting to carry out a large campaign of numerical simulations. Indeed, the cavity collapse, cavity reversal, jet dynamics, and end pinching are very complex phenomenon and their dynamics involve a high dependency on the local gradient concentration. In simulations Marangoni stresses can be turned off while surfactant-induced lowering of surface tension can be retained, thereby determining which of the two effects is the dominant

mechanism by which surfactants affect the flow [37]. However, simulations would also enable a statistical characterization of the drop production [24,48] as it seems to be very sensitive to the experimental conditions and probably to the initial conditions. Finally, in any way, the surfactant concentration needs to be taken into account in the experiments and simulations to improve the prediction of a real bubble bursting spray as the sea spray.

[1] C. Garrett, M. Li, and D. Farmer, The connection between bubble size spectra and energy dissipation rates in the upper ocean, J. Phys. Oceanogr. **30**, 2163 (2000).

[2] G. B. Deane and M. D. Stokes, Scale dependence of bubble creation mechanisms in breaking waves, Nature (London) **418**, 839 (2002).

[3] K. A. Prather, T. H. Bertram, V. H. Grassian, G. B. Deane, M. D. Stokes, P. J. DeMott, L. I. Aluwihare, B. P. Palenik, F. Azam, J. H. Seinfeld *et al.*, Bringing the ocean into the laboratory to probe the chemical complexity of sea spray aerosol, Proc. Natl. Acad. Sci. USA **110**, 7550 (2013).

[4] L. Deike, W. K. Melville, and S. Popinet, Air entrainment and bubble statistics in breaking waves, J. Fluid Mech. **801**, 91 (2016).

[5] L. Deike, Mass transfer at the ocean–atmosphere interface: The role of wave breaking, droplets, and bubbles, Annu. Rev. Fluid Mech. **54**, 191 (2021).

[6] D. C. Blanchard and L. D. Syzdek, Film drop production as a function of bubble size, J. Geophys. Res. **93**, 3649 (1988).

[7] H. Lhuissier and E. Villermaux, Bursting bubble aerosols, J. Fluid Mech. **696**, 5 (2012).

[8] D. E. Spiel, More on the births of jet drops from bubbles bursting on seawater surfaces, J. Geophys. Res. **102**, 5815 (1997).

[9] E. Ghabache, A. Antkowiak, C. Josserand, and Thomas Séon, On the physics of fizziness: How bubble bursting controls droplets ejection, Phys. Fluids **26**, 121701 (2014).

[10] E. Ghabache and T. Séon, Size of the top jet drop produced by bubble bursting, Phys. Rev. Fluids **1**, 051901 (2016).

[11] C F. Brasz, C. T. Bartlett, P. L. L. Walls, E. G. Flynn, Y. E. Yu, and J. C. Bird, Minimum size for the top jet drop from a bursting bubble, Phys. Rev. Fluids **3**, 074001 (2018).

[12] A. M. Gañán-Calvo, Revision of Bubble Bursting: Universal Scaling Laws of Top Jet Drop Size and Speed, Phys. Rev. Lett. **119**, 204502 (2017).

[13] F. J. Blanco-Rodríguez and J. M. Gordillo, On the sea spray aerosol originated from bubble bursting jets, J. Fluid Mech. **886**, R2 (2020).

[14] F. Veron, C. Hopkins, E. L. Harrison, and J. A. Mueller, Sea spray spume droplet production in high wind speeds, Geophys. Res. Lett. **39**, L16602 (2012).

[15] E. R. Lewis and S. E. Schwartz, *Sea Salt Aerosol Production: Mechanisms, Methods, Measurements, and Models* (American Geophysical Union, Washington, DC, 2004).

[16] F. Veron, Ocean spray, Annu. Rev. Fluid Mech. **47**, 507 (2015).

[17] G. de Leeuw, E. L. Andreas, M. D. Anguelova, C. W. Fairall, E. R. Lewis, C. O'Dowd, M. Schulz, and S. E. Schwartz, Production flux of sea spray aerosol, Rev. Geophys. **49**, RG2001 (2011).

[18] L. Deike and W. K. Melville, Gas transfer by breaking waves, Geophys. Res. Lett. **45**, 10 (2018).

[19] D. C. Blanchard, The electrification of the atmosphere by particles from bubbles in the sea, Progr. Oceanogr. **1**, 73 (1963).

[20] T. Séon and G. Liger-Belair, Effervescence in champagne and sparkling wines: From bubble bursting to droplet evaporation, Eur. Phys. J.: Spec. Top. **226**, 117 (2017).

[21] L. Duchemin, S. Popinet, C. Josserand, and S. Zaleski, Jet formation in bubbles bursting at a free surface, Phys. Fluids **14**, 3000 (2002).

[22] A. Berny, L. Deike, T. Séon, and S. Popinet, Role of all jet drops in mass transfer from bursting bubbles, Phys. Rev. Fluids **5**, 033605 (2020).

[23] A. M. Gañán-Calvo, Scaling laws of top jet drop size and speed from bubble bursting including gravity and inviscid limit, Phys. Rev. Fluids **3**, 091601(R) (2018).
[24] A. Berny, S. Popinet, T. Séon, and L. Deike, Statistics of jet drop production, Geophys. Res. Lett. **48**, 10 (2021).
[25] O. Wurl, E. Wurl, L. Miller, K. Johnson, and S. Vagle, Formation and global distribution of sea-surface microlayers, Biogeosciences **8**, 121 (2011).
[26] S. Poulain, E. Villermaux, and L. Bourouiba, Ageing and burst of surface bubbles, J. Fluid Mech. **851**, 636 (2018).
[27] D. B. Shaw and L. Deike, Surface bubble coalescence, J. Fluid Mech. **915**, A105 (2021).
[28] B. Néel and L. Deike, Collective bursting of free-surface bubbles, and the role of surface contamination, J. Fluid Mech. **917**, A46 (2021).
[29] B. Néel, M. A. Erinin, and L. Deike, Role of contamination in optimal droplet production by collective bubble bursting, Geophys. Res. Lett. **49**, e2021GL096740 (2022).
[30] R. L. Modini, L. M. Russell, G. B. Deane, and M. D. Stokes, Effect of soluble surfactant on bubble persistence and bubble-produced aerosol particles, J. Geophys. Res.: Atmos. **118**, 1388 (2013).
[31] P. K. Quinn, D. B. Collins, V. H. Grassian, K. A. Prather, and T. S. Bates, Chemistry and related properties of freshly emitted sea spray aerosol, Chem. Rev. **115**, 4383 (2015).
[32] C. R. Constante-Amores, L. Kahouadji, A. Batchvarov, S. Shin, J. Chergui, D. Juric, and O. K. Matar, Dynamics of a surfactant-laden bubble bursting through an interface, J. Fluid Mech. **911**, A57 (2021).
[33] V. Thominet, C. Stenvot, and D. Langevin, Light scattering study of the viscoelasticity of soluble monolayers, J. Colloid Interface Sci. **126**, 54 (1987).
[34] J. D. Berry, M. J. Neeson, R. R. Dagastine, D. Y. C. Chan, and R. F. Tabor, Measurement of surface and interfacial tension using pendant drop tensiometry, J. Colloid Interface Sci. **454**, 226 (2015).
[35] Y. Toba, Drop production by bursting of air bubbles on the sea surface (ii) theoretical study on the shape of floating bubbles, J. Oceanogr. Soc. Japan **15**, 121 (1959).
[36] M. Poujol, R. Wunenburger, F. Ollivier, A. Antkowiak, and J. Pierre, Sound of effervescence, Phys. Rev. Fluids **6**, 013604 (2021).
[37] P. M. Kamat, B. W. Wagoner, S. S. Thete, and O. A. Basaran, Role of marangoni stress during breakup of surfactant-covered liquid threads: Reduced rates of thinning and microthread cascades, Phys. Rev. Fluids **3**, 043602 (2018).
[38] H. Manikantan and T. M. Squires, Surfactant dynamics: Hidden variables controlling fluid flows, J. Fluid Mech. **892**, P1 (2020).
[39] J. Lucassen, Dynamic properties of free liquid films and foams, in *Anionic Surfactants* (Marcel Dekker, New York, NY, 1981), pp. 217–265.
[40] C. Stubenrauch and R. Miller, Stability of foam films and surface rheology: An oscillating bubble study at low frequencies, J. Phys. Chem. B **108**, 6412 (2004).
[41] P. T. McGough and O. A. Basaran, Repeated Formation of Fluid Threads in Breakup of a Surfactant-Covered Jet, Phys. Rev. Lett. **96**, 054502 (2006).
[42] J. R. Lu, I. P. Purcell, E. M. Lee, E. A. Simister, R. K. Thomas, A. R. Rennie, and J. Penfold, The composition and structure of sodium dodecyl sulfate-dodecanol mixtures adsorbed at the air-water interface: A neutron reflection study, J. Colloid Interface Sci. **174**, 441 (1995).
[43] C.-H. Chang and E. I. Franses, Adsorption dynamics of surfactants at the air/water interface: A critical review of mathematical models, data, and mechanisms, Colloids Surf., A **100**, 1 (1995).
[44] I. Cantat, S. Cohen-Addad, F. Elias, F. Graner, R. Höhler, O. Pitois, F. Rouyer, and A. Saint-Jalmes, *Foams: Structure and Dynamics* (Oxford University Press, Oxford, UK, 2013).
[45] K. Kinoshita, E. Parra, and D. Needham, Adsorption of ionic surfactants at microscopic air-water interfaces using the micropipette interfacial area-expansion method: Measurement of the diffusion coefficient and renormalization of the mean ionic activity for SDS, J. Colloid Interface Sci. **504**, 765 (2017).
[46] L. Deike, E. Ghabache, G. Liger-Belair, A. K. Das, S. Zaleski, S. Popinet, and T. Séon, Dynamics of jets produced by bursting bubbles, Phys. Rev. Fluids **3**, 013603 (2018).

[47] E. Ghabache, G. Liger-Belair, A. Antkowiak, and T. Séon, Evaporation of droplets in a champagne wine aerosol, Sci. Rep. **6**, 25148 (2016).

[48] A. Berny, L. Deike, S. Popinet, and T. Séon, Size and speed of jet drops are robust to initial perturbations, Phys. Rev. Fluids **7**, 013602 (2022).

[49] J. M. Gordillo and J. Rodríguez-Rodríguez, Capillary waves control the ejection of bubble bursting jets, J. Fluid Mech. **867**, 556 (2019).